Mol Breeding (2009) 23:239–257
DOI 10.1007/s11032-008-9229-8

Altering *FVE/MSI4* results in a substantial increase of biomass in *Arabidopsis*—the functional analysis of an ontogenesis accelerator

Patrice Morel · Christophe Tréhin · Stéphanie Breuil-Broyer · Ioan Negrutiu

Received: 19 December 2007 / Accepted: 8 October 2008 / Published online: 23 October 2008

Abstract *FVE/MSI4,* a highly conserved gene through evolution, is considered a classical flowering time gene from the autonomous pathway in *Arabidopsis thaliana*. Our work provides complementary, yet distinct, evidence that mutations *in FVE/MSI4* have highly pleiotropic effects on plant architecture and organ production and growth, indicating an overall role in reprogramming the genome. First, this is illustrated by the fact that *fve* mutants and transgenic versions of the gene show no morphological aberrations while living, on average, twice as long and producing more biomass and seeds than the wild type. For example, depending on the photoperiod, the vegetative biomass in the mutants is increased three- to eightfold. *FVE/MSI4* can therefore be considered a multifactor component of biomass and yield. Second, the gene functions primarily at the shoot apical meristem, acting to calibrate its overall cell proliferation activity and organ initiation. At the same time, *FVE/MSI4* regulates cell growth during organ formation mainly by modulating the timing of proliferation—differentiation transition and that of endoreduplication. *FVE/MSI4* is an accelerator of ontogenesis. The function of the gene is to scale-down meristem activities, while accelerating developmental transitions and cellular differentiation. Genes of the kind are ideal tools in biotech for engineering biomass and yield according to geographical or climate constraints. The results enhance our understanding on the role epigenetic components of the genome, such as *FVE/MSI4,* play in adaptation and biomass calibration. They also illustrate the kind of functional characterization biotech applications might require during the first steps of product development.

Keywords *Arabidopsis* · Biomass · Lifespan · Meristems · Organ growth · Ontogenesis accelerator · *FVE/MSI4* · *TFL2/LHP1*

Introduction

The development of seed plants is a striking example of a highly orchestrated series of biological processes in space and time during which the control of cell division and growth plays a pivotal role (Meyerowitz 1997; Hemerly et al. 1999; Vernoux et al. 2000; Sharma and Fletcher 2002). This is the case, for example, for lateral organ initiation (Vernoux et al. 2000), floral transition (Mouradov et al. 2002; Simpson and Dean 2002; Jack 2004) or apical and flower meristem formation (Sharma and Fletcher

Electronic supplementary material The online version of this article (doi:10.1007/s11032-008-9229-8) contains supplementary material, which is available to authorized users.

P. Morel · C. Tréhin · S. Breuil-Broyer · I. Negrutiu (✉)
Laboratoire de Reproduction et Développement des Plantes, Université de Lyon, CNRS, INRA, UMR 5667, Ecole Normale Supérieure, 46, Allée d'Italie, 69347 Lyon Cedex 07, France
e-mail: ioan.negrutiu@ens-lyon.fr

2002; Krizek and Fletcher 2006), for which models and regulatory pathways have been proposed.

In the case of flowering time, its control is presently understood as a networking of several well-established regulatory pathways, including photoperiod, vernalization or autonomous pathways (Mouradov et al. 2002; Jack 2004; Quesada et al. 2005). Several of the corresponding genes operate to control flowering by limiting the accumulation of the floral repressor *FLOWERING LOCUS C* (*FLC*), a critical regulator of the switch to flowering (Fig. 1; Mouradov et al. 2002; Simpson and Dean 2002; Michaels et al. 2003; Bäurle and Dean 2006). In this process, the autonomous pathway holds a critical and peculiar position, integrating external and internal cues. The genes within this pathway promote flowering by preventing the accumulation of *FLC* mRNA. They constitutively activate flowering via transcriptional and post-transcriptional regulated processes, in particular chromatin remodeling and RNA processing (reviewed by Simpson 2004; He and Amasino 2005; Quesada et al. 2005; Bäurle and Dean 2006).

Despite this wealth of molecular data, we lack a comprehensive view on cellular processes (meristem activity, cell growth control) during such a critical developmental transition (also see Komeda 2004). This understanding is important for an additional reason: flowering time is a significant factor in plant productivity. In cereals and other crops, flowering time is key to yield optimization and stability, and therefore its molecular dissection has been initiated in the recent past in rice, maize, etc. (reviewed by Koorneeff et al. 2004).

To address this question, we extended the functional analysis of *FVE/MSI4,* an autonomous pathway gene and a plant-specific member of the MSI WD-40 subfamily (Yu et al. 2000), acting as a component of HDAC complexes and as such regulating the acetylation levels at the *FLC* locus (Ausin et al. 2004). Using a new allele generated by T-DNA insertion mutagenesis, we analyze the pleiotropic effects of mutations in this gene by studying combined alterations in meristem activity and in cellular aspects of organ growth and differentiation. We demonstrate that *FVE/MSI4* is primarily a meristem regulator where it operates to calibrate growth rates. Furthermore, *FVE/MSI4* is expressed in growing organs where it regulates the timing and speed of differentiation. We present evidence that this is achieved via

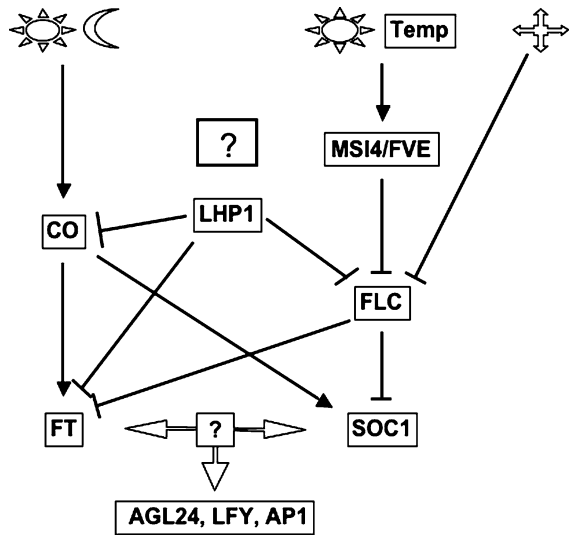

Fig. 1 The role of *FVE/MSI4* in flowering time control. Schematic representation of three of the flowering induction pathways, namely photoperiod (sun and moon), autonomous (small sun and ambient temperature) and vernalization (snowflake). There are at least two levels of integration of flowering signals: one is *FLC*, the assigned target of the autonomous pathway. *FVE/MSI4* is a member of the pathway and as such known to repress *FLC*. The downstream level of integration involves *SOC1* and *FT*, on which *FLC* acts as repressor. *FT* and *SOC1*, in turn, act on "mediators" such as *AGL24*, *LFY, APETALA1 (AP1),* which promote flowering (Simpson and Dean 2002; Yu et al. 2002). The balance of *FT* and *SOC1* is differentially controlled through the antagonistic effects of several upstream regulators (Samach et al. 2000; Kobayashi et al. 1999; Kotake et al. 2003). Genetic and molecular evidence (Gaudin et al. 2001; Kotake et al. 2003; Takada and Goto 2003; Mylne et al. 2006 and our work) position *TFL2/LHP1* upstream of *FLC* and *FT*, and define *TFL2/LHP1* as a key repressor of *FT*. However, *TFL2/LHP1* has not been assigned to an established flowering time pathway. *TFL2/LHP1* has been shown to be a potent repressor of *CO* (Gaudin et al. 2001) and *FT*, being required in the maintenance of *FLC* silencing in vernalized plants (Mylne et al. 2006) and for the maintenance of transcriptional repression of flower homeotic genes (Kotake et al. 2003; Nakahigashi et al. 2005)

interactions with another major epigenetic regulator, *TERMINAL FLOWER2* (*TFL2*), a gene coding for the *HETEROCHROMATIN PROTEIN1* (*LHP1*) homologue. Taken together, the results suggest that *FVE/MSI4* operates as a connectivity factor integrating meristem and organ growth throughout adult phase transitions, of which flowering time is the most conspicuous transition. The result is a coordinated architecture, biomass and life-span. The potential biotech applications in biomass calibration are discussed.

Materials and methods

Plant material and growth conditions

All the *A. thaliana* plants used in this work belong to the W*s*, L*er* and Col-0 ecotypes. *fve-1* and *fve-2* late flowering mutant lines were obtained from the Nottingham Arabidopsis Stock Center (NASC). Tagged lines were identified in collections from INRA Versailles, France and Syngenta, USA by PCR screens or flag base searches. Promoter line insertions (four candidates) in *FVE/MSI4* had no obvious phenotype, while insertions mapping to the 3′ half of *FVE/MSI4* (FLAG line DOL3 and GARLIC line 1167 E05) exhibited late flowering phenotypes.

In this study, we concentrated our efforts on the DOL3/*fve-6* (W*s* background) line. The *fve-6* mutant was screened by PCR using primers corresponding to the right and left borders of the T-DNA and the *FVE/MSI4* gene. Southern and segregation analyses revealed that the DOL3 line contains three independent T-DNA insertions. A plant carrying only one T-DNA insertion genetically linked to *FVE/MSI4* disruption was isolated after three backcrosses to W*s*. All analyses were carried out with plants backcrossed four times.

Crosses between *fve-6* and *fve* or *fca* mutant alleles indicated that *fve-6*, *fve-1* and *fve-2* mutations belong to the same complementation group (data not shown). Like *fve-1* and *fve-2* (Martinez-Zapater et al. 1995), *fve-6* behaved as a semi-dominant mutant in F1 under short day conditions (not shown).

The *CycB1;1:CDBGUS* reporter line, FA4C, has been described previously (Colon-Carmona et al. 1999). In this construct, the cyclin-destruction-box (CDB) of *CycB1;1* is fused in frame to GUS, causing the protein to be degraded at the end of mitosis, allowing visualization of cell-cycle progression by staining for GUS activity. Cyclin marker line *CycB1;1:GUS* was a gift from Dirk Inzé (Ferreira et al. 1994). *flc-3* (Col-0) and tfl2-3 (Col-0) were a gift from Hao Yu and *lhp1* (W*s*) was a gift from Valerie Gaudin. *fve-1, 2* and *fca1* (L*er*) were obtained from the NASC. Plants were grown under short-day (8-h light) or long-day (16-h light) conditions (Gro-Lux, Sylvania). For vernalization treatments, seeds were sown in pots, germinated in the dark, and exposed to 4°C in the dark over 4 weeks.

Plasmid constructs and plant transformation

cDNAs of *FVE/MSI4* (At2g19520), *MSI5* (At4g29730) and *SLY1* of *S. latifolia* (GenBank Accession no. Y18518) were amplified by PCR using high fidelity *PfuTurbo* DNA polymerase (Stratagene) and cloned downstream of the *35S* promoter into a derivative of the binary vector pGPTV-HPT (Becker et al. 1992).

All plasmids were introduced into *Agrobacterium tumefaciens* strain EHA105 by electroporation and transformed into W*s* plants by the vacuum-infiltration method (Bechtold et al. 1993). Transgenic seedlings were selected by resistance to hygromycin B (30 μg ml^{-1}) on MS (Sigma) plates containing 3% sucrose, before they were transplanted to soil. The presence of the transgene was verified by PCR. Unless otherwise stated, all manipulations were performed by using standard molecular methods (Ausubel et al. 1993).

Flowering time, leaf number, biomass and phenotypic characteristics

Flowering time was measured as number of days from seed germination to the opening of the first flower. Rosette leaf numbers were counted and vegetative biomass measured when the first flower was formed on the main inflorescence. An additional time point for measuring biomass was taken at the first silique stage. Fresh and dry weight were measured at harvest and on samples dried at 70°C for 48 h, respectively.

Phase change analysis

Leaves were classified according to blade shape, petiole length, trichome production on adaxial versus abaxial side and leaf serration as juvenile, early and late adult leaves. Developmental stages were defined according to these criteria.

Northern blot and reverse transcription (RT)-PCR analyses

RNA was isolated from plants using the TRIZOL method. After treatment with DNaseI, first-strand cDNA was prepared from 5 μg of total RNA with the Superscript RT II kit (Invitrogen) and oligo $(dT)_{18}$

according to the manufacturer's instructions. Aliquots of the generated cDNA, which equaled 50 ng total RNA, were used as template for PCR amplification with gene specific primers. After amplification, 10 µl of the RT-PCR products were separated on an agarose gel, stained with ethidium bromide and quantified using NIH image program.

Sequences of gene-specific primers used for RT-PCR

Gene	Forward primer	Reverse primer
CYCD3	TTCCCGGGAATGCTCTGAGCCAAAAC	AAGAGCTCAAACGGGTAAAGCTTAATAC
GAPDH	GTAGCCCCACTCGTTGTCGTA	AGGGTGGTGCCAAGAAGGTTG
FLC	CCCCATATGGGAAGAAAAAAACTAG	CCCGGATCCCTAATTAAGTAGTGGGAG
flc3	GCTTCTTCACGACATTGTTCT	GTAGCAAAGACGCTCGTCATG
FT	ACTATATAGGCATCATCACCGTTCGTTACTCG	ACAACTGGAACAACCTTTGGCAATG
LFY	ACCAAGGTGACGAACCAAGTATTC	TGGAGAGCGTAACAGTGAACGTAG
LHP1	CGATTGTACTTGAGATGTTGCT	GGAGGTGGAAGTGGAGAGTCG
FVE/MSI4	CTCCATTTGTGAAGAAGTACAAGACCATC	AAGCTTCCTACGATCAAAC
MSI5	ACAACGAGTCTCAGTTAC	GTAAGGTTTCGGCGGTCA
SOC1	AATATGCAAGATACCATAGATCG	TCTTGAAGAACAAGGTAACCCAAT
TFL1	GACCCAGATGTTCCAGGTCC	CTAGCGTTTGCGTGCAGCGG
tfl2-3	GGCAAGGTTCAGTATCTAATT	TGTCCACCAATGCTTCCTTCC

Western blot analysis

A cross-reacting antibody against SLY1, the FVE/MSI4 ortholog in *S. latifolia*, was generated and employed as reported in Delichère et al. (1999).

Glucuronidase (GUS) assays

Histochemical assays for GUS expression analysis were performed according to Hemerly et al. (1993).

In situ RNA hybridization

In situ detection of mRNA on paraffin-embedded tissues of *A. thaliana* was performed as described (de Almeida Engler et al. 2001). Anti-dioxigenin alkaline phosphatase Fab fragment (Boehringer) and 0,8-nm colloidal gold-conjugated anti-dioxigenin antibodies (Boehringer) were used as markers.

Specific non-transcribed regions of *FVE/MSI4* and *MSI5* genes were amplified by PCR from cDNA with the 5′-GAGTAAAGAAAACCCATTGTC-3′ and 5′-AGGTTCAGGCCAAGTATTGA-3′ or 5′-GTCTT GAGGAAGCAATCC-3′ and 5′-TCAGGGACACA TGAGTCA-3′ primers, respectively, and cloned in plasmid pGEMTeasy (Promega). The pGEMT-*FVE/MSI4* vector was used as template for both 400-bp antisense (SP6 RNA polymerase) and sense (T7 RNA polymerase) probes. Similarly, *MSI5* 500 bp antisense and sense probes were generated from pGEMT-MSI5 vector.

Cell size and number measurements

For the observation of epidermal cells, the distal portion of the leaf epidermis was sampled, fixed in paraformaldehyde and cleared by immersion in a mixture of ethanol and acetic acid (7:1). In flowers, the distal portion of the petal epidermis was analyzed because it has cells that are diploid and uniform in size (Mizukami and Fischer 2000). For statistical analysis, images were digitized with a UMAX scanner (UMAX Technologies) and were analyzed by using the NIH IMAGE program (http://rsb/info.nih.gov/nih-image).

DAPI staining

DNA fluorochrome 4′,6-diamidino-2-phenylindole (DAPI) at 0.5 µg ml^{-1} in Vectashield (Vector Laboratories) was used to stain nuclear contents on paraffin-embedded inflorescences of *A. thaliana*. The

fluorescence patterns were examined with a Zeiss Axioplan microscope. Statistical calculations were performed with Microsoft EXCEL program. Mathematical calculations were performed according to Lentner (1982).

Flow cytometric analysis

Plants were chopped with a razor blade in 500 µl of 45 mM $MgCl_2$, 30 mM sodium citrate, 20 mM 3-(*N*-morpholino)propanesulfonic acid pH 7 and 0.1% Triton X-100 (Galbraith et al. 1991). The supernatant was filtered over a 30 µm mesh, and 1 µl of Hoechst from a stock of 1 mg per ml was added. The nuclei were analyzed with the BRYTE HS flow cytometer and the WinBryte software (Bio-Rad).

Cell proliferation analysis

Primary *A. thaliana* inflorescences were cut 2.5 cm from the top and soaked in the BrdU solution (Sigma, 2 mg per ml). After vacuum infiltration for 10 min, soaking was continued for 2, 4, 10, 12, 16 and 20 h. Incorporation of BrdU in replicating DNA was detected by monoclonal anti-BrdU antibody (Beckton) on paraffin-embedded tissues. Tissues were mounted in Entellan (Merck) and observed with a Zeiss Axioplan microscope.

Results

Alleles in different ecotypes are late flowering and exhibit a strong increase in organ number and overall biomass

Mutations in *FVE/MSI4* represent an allelic series, with *fve-1* and *fve-2* (Ler ecotype) containing amino acid substitutions in exon 3, and *fve-3, fve-4* (Ler; Ausin et al. 2004) and *acg1* (Col ecotype; Kim et al. 2004), hereafter called *fve-5*, resulting from stop codons in the 5′-half of the gene. Here we report on a new allele named *fve-6*. The *fve-6* allele (Ws ecotype) was generated by a T-DNA insertion in the *FVE/MSI4* gene. The T-DNA left border exactly matches the limit of the 10th intron and the 11th exon of the *FVE/MSI4* gene. RACE-PCR amplification and sequencing of the fragments generated from the mutant plant suggested the synthesis of a chimeric *FVE/MSI4* transcript encoding a truncated and altered FVE/MSI4 protein (i.e. 167 amino acids at the level of the last two WD domains are replaced in frame by a 17 amino acid peptide, KSKLRKETLQHGLVAKL, encoded by the T-DNA).

The primary phenotype of all *fve* alleles in homozygous mutant plants was a delay in the transition to flowering under various light regimes and an increase in the rosette leaf number, irrespective of ecotype and protein alterations (amino acid substitutions or protein truncations at the N-ter or C-ter of the protein). F1 plants show a semi-dominant phenotype. Table 1 illustrates the morphological analysis with *fve-6*, but similar results were obtained with *fve-1* and *fve-2* (see below). In the mutant, the leaves were initiated faster (higher plastochron values), their number roughly doubled in the rosette and they were larger as compared with the wild type. During the reproductive stage, mutant plants had more co-florescences, produced more and larger flowers, and had an increased seed weight.

By summing up the increase in various organ and plant architecture traits as calculated from Table 1 (number and size of rosette leaves, number of secondary inflorescences, silique number), we estimated that the vegetative and reproductive biomass would be increased several fold in the mutants. Based on these estimates, we evaluated the accumulation of vegetative biomass in wild type and mutant backgrounds under the two standard light regimes. The results show (Table 2) that the mutants produced much larger amounts of biomass in long days (LD): fresh weight and dry weight per time unit were systematically increased by factors varying from 6 to 9. The equivalent increase in biomass was less pronounced under short days (SD, two- to fivefold increase). In the two ecotypes tested, the effect of the light regime (SD/LD) on vegetative biomass increase varied from 1.5 to 3.4, which is less than the gain in biomass due to mutations in *FVE/MSI4*. Since the biomass increase was comparable in fresh and dry weight samples, we hypothesize that the increase in biomass is essentially due to dry matter accumulation rather than water accumulation.

Seed production alone had roughly doubled as estimated by the number of siliques and secondary inflorescences produced, but more detailed and systematic observations are needed for silique and

Table 1 Morphological trait comparison between wild type (Ws) and *fve-6* mutant under two different light regimes

Light regime	Plant line	Flowering time (days)	Leaf number	Plastochron[a] (leaves/week)	Rosette size (cm)	Secondary Inflorescences[b]	Flower weight[c] (mg)	Silique number	Seed weight (mg/1,000 seeds)
LD	Ws	38 (1.5)	18.5 (2)	2.8	8.5 (0.7)	2.4 (0.5)	1.6 (0.14)	79 (25)	13 (1.4)
	fve6	77 (8)	51 (0.9)	4.5	11.2 (1.1)	4.2 (1)	2 (0.25)	185 (57)	16.5 (0.7)
SD	Ws	77 (2)	38 (2)	3.5	10.2 (0.8)	4.5 (0.6)	1.7 (0.17)	153 (23)	15 (0.4)
	fve6	97 (6)	71 (4)	5.25	12.2 (1)	6 (0.8)	2.4 (0.40)	215 (34)	17 (0.4)

Standard errors are given in brackets

P-values were very significant ($P < 0.01$) or highly significant ($P < 0.001$) for all traits. *P*-values ranged from 0 to 0.0034

[a] Plastochron (leaf production rate) was measured at various times during the year with similar results. Those presented here are based on weekly measurements

[b] Indicates reduced apical dominance for the main shoot and/or that flowers are replaced by shoots, a mark of delayed transition from inflorescence to flower formation

[c] 80–100 flowers measured as lots of 5. Similar increase in flower weight was recorded in another autonomous pathway, late flowering mutant, *fca*

Leaf, flower and silique observations did not reveal alterations in phyllotaxy

seed traits. Seed weight per se increased, respectively, by 26 and 13% in LD versus SD batches.

FVE/MSI4 is predominantly expressed in actively dividing cells

The cellular expression pattern of *FVE/MSI4* is not known. While RT-PCR analysis showed that the gene was expressed in all tissues analyzed (Fig. 2a; also see Ausin et al. 2004), in situ hybridization (Fig. 2b) revealed that *FVE/MSI4* was strongly expressed in SAMs, leaf primordia (more strongly in the adaxial domain), flower meristems (FM) and floral organ primordia, including placenta and ovules. Overall, *FVE/MSI4* is expressed in a great variety of organs and cell types, being apparently most abundant in actively dividing cells. These results are in agreement with available global expression data for all genes (Genevestigator source, Zimmermann et al. 2004); Gene Chronologer, Gene Atlas and Digital Northern were searched and indicated two expression peaks, one corresponding to flowering transition and the second to seed formation/maturation—seedling stages (including the root tip). It is therefore expected that *FVE/MSI4* could operate, in addition to flowering time control, in other developmental processes, before and after flowering.

Miss- and over-expression of the gene indicate that *FVE/MSI4* is rate limiting

Using primers complementary to *FVE/MSI4* sequences upstream from the truncation site, low but reproducible levels of gene expression were detected in the *fve-6* mutant during all developmental stages, representing an average of 40% of wild type levels (Fig. 2a). We used as an additional control the expression profile of *MSI5*, a highly similar paralog of FVE/MSI4 (over 85% identity at nucleotide level; Hennig et al. 2003) to show that the *fve-6* mutation had a gene-specific effect at transcriptional level.

Thus, *fve-6* is not a knock-out, the mutant producing a transcript which is altered both qualitatively and quantitatively, the presence of a truncated protein being confirmed by western blot analysis (Fig. 3a, lanes 1 and 2). For comparison, mutant or ectopic forms of the MSI4 protein as produced by *fve-1* and *fve-2* alleles or by transgenic plants are shown in Fig. 3a (lanes 4, 5 and 6-9, respectively). In

Table 2 Vegetative biomass accumulation in wild type and *fve* mutants

Light regime and stage	Plant line	Leaf number	Days to stage	FW (g)	Fold FW/ time	DW (mg) Bulk 12 pl.	Fold DW/ time	Average increase
LD	Ler	10 (1.2)	34 (1.4)	0.1 (0.03)		9.3		8×
First flower	*fve1*	28 (2.6)	53 (0.9)	1.4 (0.2)	9×	129	9×	
	fve2	56 (9.3)	68 (1.8)	1.8 (0.4)	9×	304	**16×**	
	Ws	11 (0.7)	31 (0.9)	0.14 (0.03)		15		
	fve6	29 (4.3)	49 (1.2)	1.7 (0.6)	7×	185	7×	
LD	Ler	14 (1.1)	39 (1.1)	0.16 (0.05)		14		7×
First silique	*fve1*	29 (3.4)	60 (0.5)	1.4 (0.3)	6×	164	7.8×	
	fve2	>60	78 (1.2)	1.8 (0.2)	5.6×	252	9×	
	Ws	13 (1)	38 (1)	0.2 (0.04)		25		
	fve6	29 (3.6)	59 (1.1)	2.2 (0.6)	7.4×	293	7×	
SD	Ler	22 (3.2)	48 (2.5)	0.37 (0.2)		41		3.5×
First flower	*fve1*	51 (5.3)	103 (2)	1.72 (0.3)	2×	219	2.5×	
	fve2	>70	108 (2)	2.25 (0.6)	2.5×	303	3.3×	
	Ws	26(2.3)	70 (1.7)	0.5 (0.1)		46		
	fve6	65 (7)	90 (1.8)	2.9 (0.9)	4.5×	335	5.6×	
SD	Ler	40 (10)	69 (1.8)	0.9 (0.4)		64		
First silique	*fve1*	57 (6.4)	109 (2)	1.9 (0.3)	1.3×	216	2.1×	2.5×
	fve2	>70	123 (2)	2.3 (0.3)	1.4×	259	2.2 ×	
	Ws	30 (2)	80 (2)	0.6 (0.1)		58		
	fve6	66 (6)	103 (2)	2.8 (0.5)	3.6×	366	4.8×	

Fresh (FW) and dry weight (DW) comparisons were performed under LD and SD light regimes and at two relatively close developmental stages (first open flower and first silique). The developmental stages were chosen in order to make two independent measurements at points of highest accumulation of vegetative biomass (maximum of leaves produced, leaf expansion terminated, biomass from secondary inflorescences, etc.). The accumulated biomass was finally evaluated on a per time unit basis, i.e., calibrated on the duration of the reference stage in the wild type and taken as a value of 1. For example, the fold-increase in biomass between a mutant and the wild type sample is divided by the ratio between the number of days to first flower (or first silique) in the mutant and the wild type. The number of days is calculated from the day seeds were transferred from cold to room temperature. Twelve plants were measured per series

Standard errors are given in brackets

Note: The bold value in column 8 has not been used to calculate the average value in column 9

Evaluation of leaf number, and hence of biomass, is somewhat biased in samples grown for longer than 10 weeks because of tissue degradation in most basal leaves. The process was more frequent in *fve1* and *fve2* samples. *fve1* and *fve2* also produced numerous small late rosette leaves

Between the first flower and first silique stage, rosette growth was most prominent in wild type samples (1.2 to 1.4-fold increase in rosette diameter) as compared to mutant samples (below 1.1)

Light regime effect on vegetative biomass increase per time unit in wild type samples has also been calculated for fresh weight

Ler, SD/LD per unit of time: 3.4-fold; Ws, SD/LD per unit of time: 1.5-fold

Tables 1 and 2 illustrate inter-experiment variations in both wild type and *fve* mutants

summary, defined point mutations or the deletion of two C-ter WD repeats produced defective proteins with similar phenotypic effects.

Ectopic expression studies were conducted with the expectation that a *35S:FVE/MSI4* construct would produce early flowering transformants in a wild type background and would complement the mutation in a *fve6* background. In the wild type background, a third of the hygromycin-resistant primary transformants (with single to multiple locus insertions) produced T2 progeny displaying a late flowering phenotype, the rest of the lines showing no phenotype (Fig. 3b). Thus,

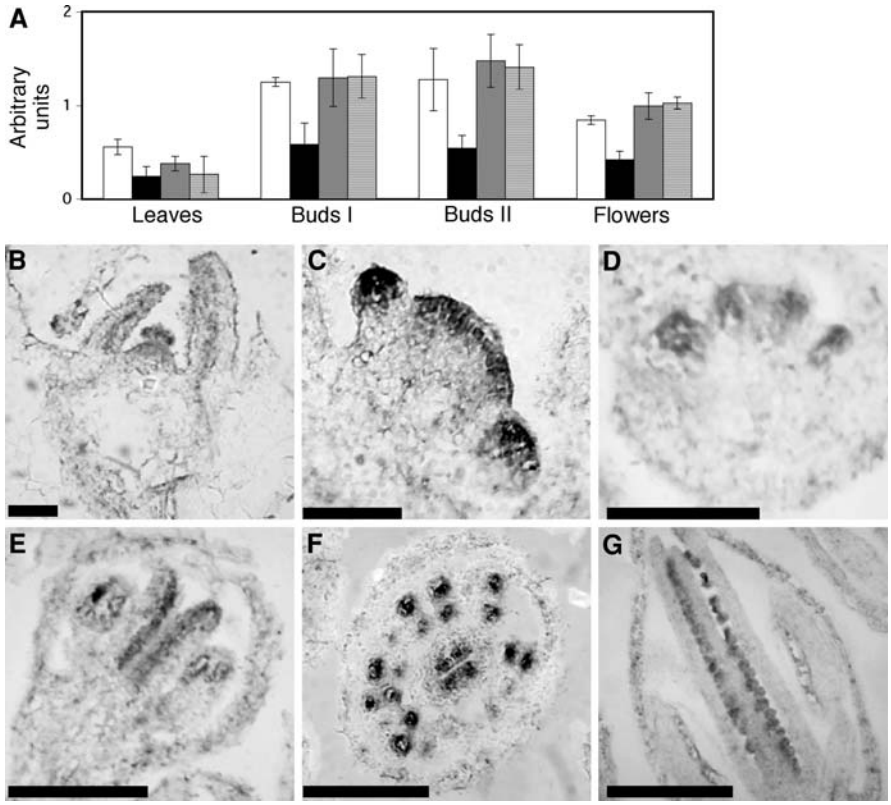

Fig. 2 Expression pattern analysis of *FVE/MSI4*. (**a**) Expression analyses by semi-quantitative RT-PCR of *FVE/MSI4* (*white* and *black bars*) and *MSI5* (*grey* and *hatched bars*) in different *Arabidopsis* tissues [rosette leaves, young inflorescences (pre- and meiotic stage buds; BudI), post-meiotic closed buds (BudII) and open flowers] of wild type (*white* and *gray bars*) and *fve-6* (*black* and *hatched bars*) plants. The level of product amplified with primers specific for each gene is expressed in arbitrary units relative to *GAPDH* in the same reaction. Data shown are the means of three replicates. Standard deviations are indicated. In the *Arabidopsis* genome, *FVE/MSI4* has a highly similar paralog, *MSI5* (over 85% identity at nucleotide level; Hennig et al. 2003) used as additional control. **b–g** *FVE/MSI4* RNA expression pattern using in situ hybridization in (**b**) the shoot apical meristem and leaf primordia; (**c**) inflorescences and floral meristems at stages 1 and 2; (**d**) early stage 5–6 flower bud; (**e**) stage 8 flower with labeled placental tissues and sporophytic tissues in anthers; (**f**) stage 10 flower bud in transverse section to show gene expression in placenta, ovule primordia, meiocytes and tapetum; (**g**) stage 12 flower with expression in early ovules. The *scale bar* represents 100 μm

mutations in *FVE/MSI4* and ectopic expression of the gene resulted in the same, late flowering, phenotype. RT-PCR analysis on seven independent T2 homozygous plants showed a range of *FVE/MSI4* transcript levels (not shown), and thus no strict correlation with the late flowering phenotype (Fig. 3b, grey bar samples). Western blot analysis confirmed the result as late flowering plants were either lacking or over-expressing the FVE/MSI4 protein (Fig. 3a, lanes 6–8). Finally, ectopic expression of *FVE/MSI4* cDNA in the *fve6* mutant did not complement the mutation and had no other phenotypic effects.

In conclusion, the late flowering phenotype observed in *fve6* mutant and wild type backgrounds could result from distinct mechanisms. In *fve6*, the disrupted *FVE/MSI4* gene gave rise to a truncated and defective FVE/MSI4 protein, which could act in the presence of the wild type version of the gene through a dominant negative effect and explain the lack of genetic complementation. In the wild type background, the observed late flowering phenotype could result from either a post-transcriptional gene silencing (PTGS) mechanism (Fig. 3a, lanes 6 and 8 show no FVE/MSI4 protein), or a dose-dependent (titration) effect of the ectopically expressed *FVE/MSI4* gene (Fig. 3a, lane 7 shows the presence of a more abundant protein amount). These results confirm previous observations at RNA level (Ausin et al.

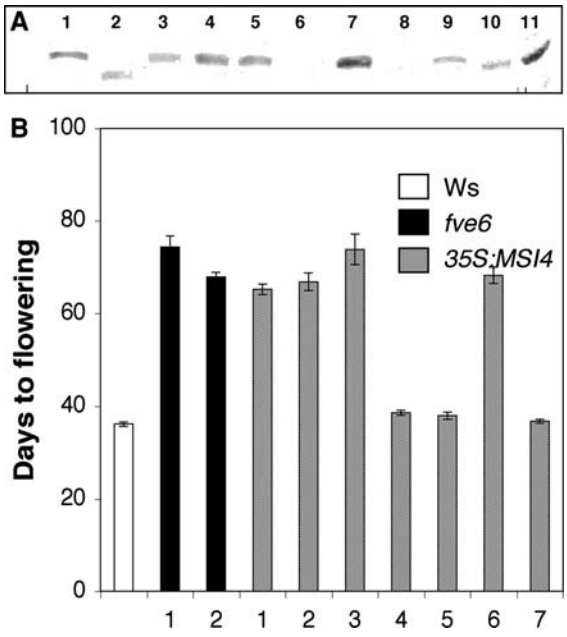

Fig. 3 Protein levels and flowering time measurements in wild type, mutants and *lines* with ectopic *FVE/MSI4* expression. **a** Western blot analysis of FVE/MSI4 accumulation in wild type, in three *fve* alleles and four *lines* expressing *35S:FVE/MSI4* in a W*s* background. (1) W*s*; (2) *fve-6*; (3) *Ler*; (4) *fve-1*; (5) *fve-2*; (6–9) *35S:FVE/MSI4* transgenic plants exhibiting late flowering in lanes 6–8 and normal flowering in lane 9; (10) SLY1 control from bacterial extracts, cf. Materials and methods; (11) FVE/MSI4 control from bacterial extracts. *Note* that the expressed *SlY1* cDNA is shorter than the *FVE/MSI4* cDNA. **b** Effects on flowering time due to altered expression of *FVE/MSI4*. In order from left to right, Ws, *fve-6* mutant (2 independent series) and *35S:FVE/MSI4* transgenics (7 lines). In the latter, lines 1 and 3 correspond to samples 6 and 8 in Fig. 3a, line 2 corresponds to sample 7 and line 4 to sample 9, respectively. All plants were grown under long days. Flowering time is expressed as the number of days to flowering. The average from 6 independent homozygous plants is shown in each case. *Error bars* indicate standard deviation

2004) and extend them at protein level, making more clear how the range of qualitative and/or quantitative modifications in gene activity can lead to one and the same phenotype: late flowering and biomass increase.

FVE/MSI4 and meristem activities

From data on gene expression and mutant phenotype, we infer that *FVE/MSI4* must act on both meristem activities and organ growth during all adult stages. We therefore decided to analyze these effects at cellular and molecular levels.

Altered *FVE/MSI4* increases meristem size and division rates

We first performed size measurements on vegetative (SAMv) and reproductive (SAMi, FM) meristems to show that the mutant meristems contain more cells. The surface area of SAMv (both apical and axillary) was approximately twice as large in the mutant as compared with the wild type (Fig. 4a). However, no significant differences in cell size were observed. Size measurements of SAMi and FM, together with DAPI staining, showed that these meristems were considerably enlarged (threefold; Fig. 4a, also see Fig. 5) and contained more cells of bigger size in the mutant as compared with the wild type. For example, a mutant SAMi contained twice as many L1 cells as the wild type. The results indicated that the mutation had more pronounced effects on meristem size during the reproductive phase.

Since the mutant exhibited larger meristems, we decided to further explore whether cell division rates were altered in the mutant meristems.

Cell division rates were examined by monitoring the incorporation of the base analogue 5-bromodeoxyuridine (BrdU) into replicating DNA. After 4 h soaking, no signal appeared in the wild type meristems (Fig. 5a), whereas active cell divisions were observed in the mutant as the majority of these cells were labeled (Fig. 5b). In the wild type, comparable patterns were only detected after 12–15 h soaking. These results showed that within SAMs and FMs of similar stage, division rates were higher in the mutant than in the wild type. In addition, the BrdU patterns coincided with the in situ expression pattern of *FVE/MSI4*, indicating that the gene is expressed in regions of active cell division.

Finally, despite the reported modifications in meristem size and activity in the mutant, no obvious changes in overall meristem organization were observed.

FVE/MSI4 and the control of organ growth

The *fve-6* mutant not only makes more organs, but these organs are also larger. To understand how *FVE/MSI4* operates at organ level, we quantified a series of cellular growth parameters in chosen organs.

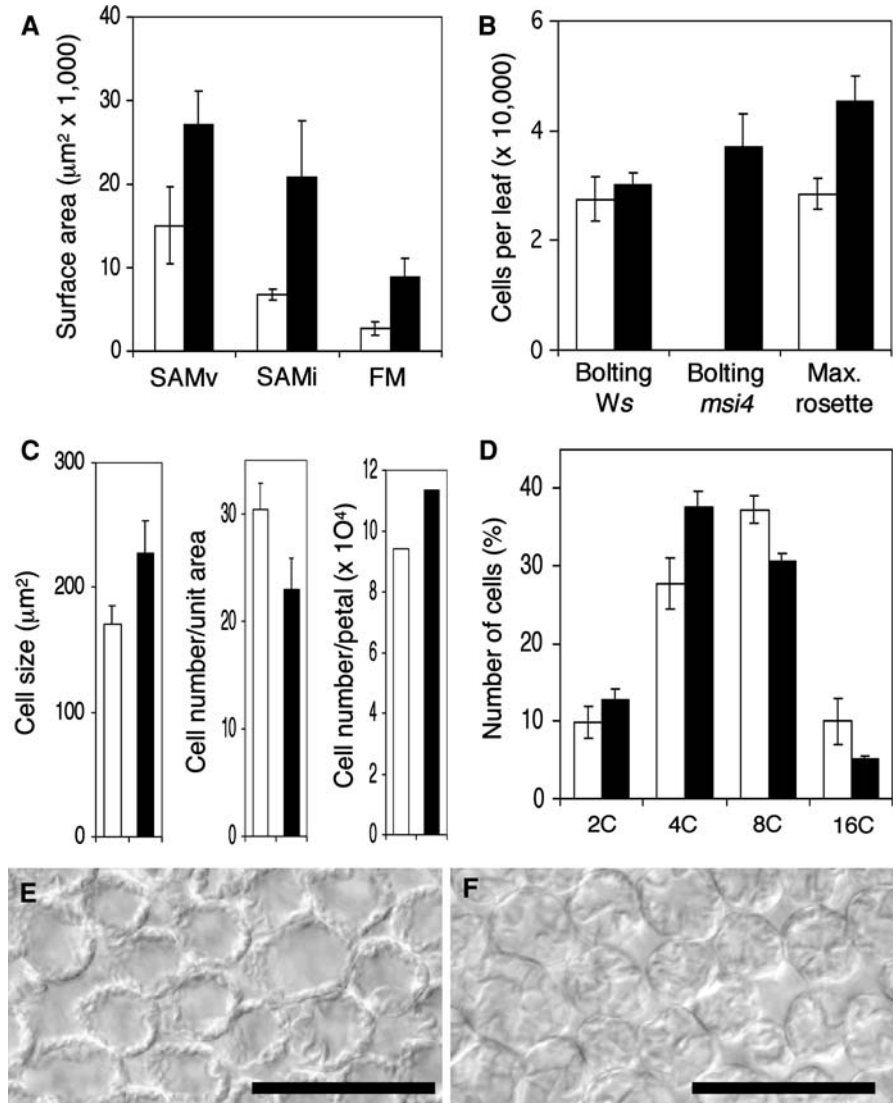

Fig. 4 Effects of the *fve-6* mutation at cellular level. **a** Comparison of SAM and FM size in W*s* (*white bars*) and *fve-6* mutant (*black bars*) plants: vegetative shoot apical meristems (SAMv), inflorescence shoot apical meristems (SAMi; first open flower stage) and floral meristems (FM). Meristematic areas were extrapolated from median longitudinal sections using calculations according to Lentner (1982). The average from at least 20 independent meristems is shown in each case. *Error bars* indicate standard deviation. **b–d** Comparison of cellular growth and differentiation parameters in W*s* (*white bars*) and *fve-6* plants (*black bars*). *Error bars* indicate standard deviation. **b** Total cell number in rosette leaves at different development stages. The three largest rosette leaves from independent plants were sampled at bolting in W*s* ("Bolting W*s*"; the plants have the same age), at bolting in the mutant (Bolting *fve-6*; the mutant at the same stage as "Bolting W*s*", therefore no wild type sample is present), and after bolting at maximum rosettes size ("Max rosette"). The number of cells per leaf was extrapolated from leaf surface calculations. The average from three leaves is shown in each case. **c** Comparison of petal growth parameters in mature flowers. **d** Measurement of endoreduplication levels. Nuclear DNA content as measured by flow cytometry in leaves harvested at equivalent developmental stages in W*s* and *fve-6* plants (12–15 leaf stage). The symbol C corresponds to the nuclear DNA content equivalent to one haploid genome. The average from 3 leaves is shown in each case. **e** and **f** Cellular differentiation is faster in the wild type as compared with the *fve-6* mutant. Are shown sub-epidermal mesophyll cells in wild type (*left*) and *fve-6* (*right*) in the three largest rosette leaves sampled at bolting in the wild type, i.e., the plants have the same age. Note that the cells in the mutant are less differentiated than in the wild type based on vacuolar size and chloroplast organization. The *scale bar* represents 50 µm

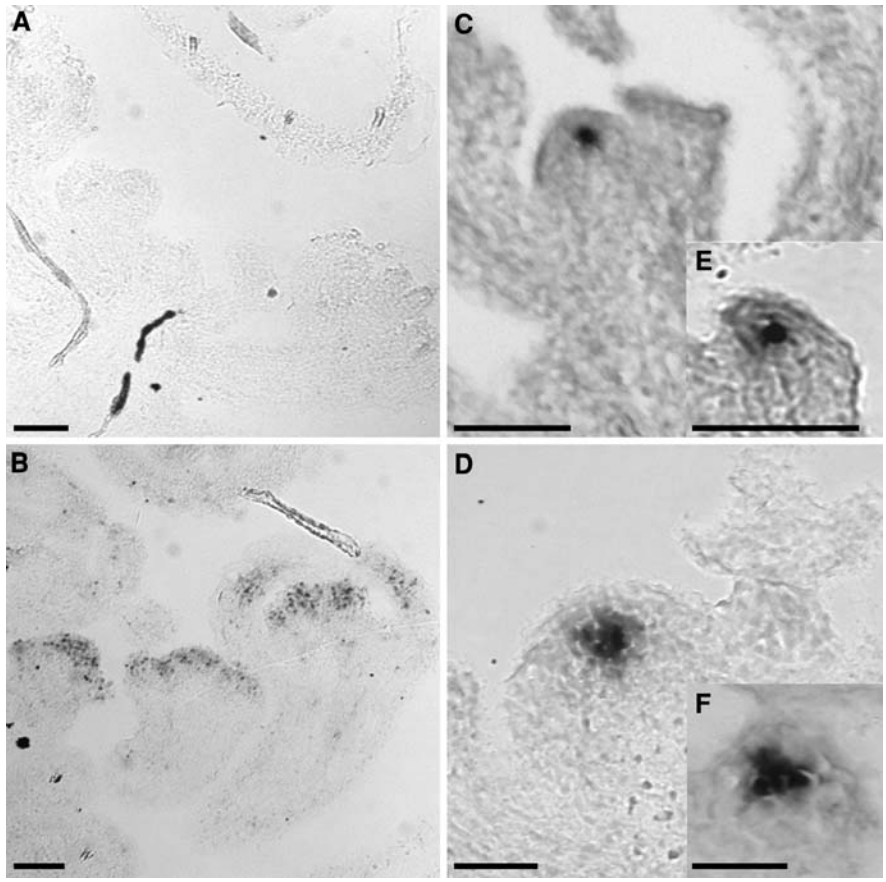

Fig. 5 Comparative proliferation activity in reproductive meristems in W*s* and *fve-6* plants. **a** and **b** Proliferation activity as measured by BrdU incorporation in W*s* (**a**) and *fve-6* (**b**) at 4 h, with no or low labeling in wild type and active incorporation in the mutant (SAM and floral FM at stages 1–3, 5/6 and 8). Flower meristems are dividing most actively. **c–f** *WUS* mRNA expression pattern in W*s* (**c**, **e**) and *fve-6* (**d**, **f**). Note that the expression domain in the mutant is proportionally enlarged, if not larger, as compared to the wild type. The expression pattern appears similar in that in the inflorescence meristem *WUS* labels a group of central cells underneath the L3, while in floral meristems, *WUS* is expressed in groups of cells underneath the L2. Inserts (**e**) and (**f**) represent stage two flower meristems. The *scale bar* represents 50 μm

Altered *FVE/MSI4* increases mature organ size by differentially altering cell number and cell size

In order to dissect out at cellular level the role of *FVE/MSI4* in organ growth control, we measured the effects of the mutation on cell number and cell size.

Larger leaves of fve-6 are due to increased cell number, despite smaller cell size

Mutant plants exhibited increased rosette and leaf size (the range is 10–25%, depending on the light regime). Mutant leaves contained more cells (1.5-fold, Fig. 4b), of smaller size (1.2-fold, not shown) than wild type. We concluded that overall leaf size is determined by a partial growth compensation mechanism (cell number vs. cell size), in which *FVE/MSI4* is involved. Since we have not measured the size of leaf primordia, we could not distinguish at what level (leaf initiation, leaf growth, or both) the compensation mechanism operates.

Oversized flowers of fve-6 are due to increased cell number and size

Flower weight data and morphological observations (Table 1 and data not shown) indicated that flower organs were larger in the mutant. We found that the

fve-6 petal size was increased by approximately 60% and that these petals had 20% more and 30% larger cells than the wild type (Fig. 4c). Thus, the overall increase in petal size was associated with both an increase in cell number and an increase in cell size. Knowing that the corresponding flower meristems were three-times larger and had larger cells in the mutant, these growth measurements indicated some growth compensation for cell number, but not for cell size.

From the combined data on leaf and petal growth we concluded that *FVE/MSI4* exerted a differential control on organ growth depending on organ type.

Altered *FVE/MSI4* increases mature organ size by modifying the timing of cell proliferation—cell differentiation transitions and by delaying endoreduplication

Subsequently we wanted to look at whether a mutated *FVE/MSI4* alters the balance between cell proliferation and endoreduplication during organ growth.

In order to assess cell cycle progression in the mutant, we evaluated *CycD3* transcript levels and *CycD3:GUS* reporter profiles. Similar results were obtained in wild type and the mutant (not shown). We concluded that the G1/S transition controls were not significantly affected in the mutant.

We subsequently crossed *fve-6* to the cell cycle reporter lines Arath;*CycB1*;1*:GUS* and Arath;*CycB1;1:CDB:GUS* (the latter contains the Cyclin-Destruction-Box fused in frame to GUS, cf. Materials and Methods). During the vegetative stage, the *fve-6* mutant showed no differences or weak differential GUS accumulation in the veins (Supplemental Fig. 1a). During the reproductive phase, a much stronger and extended GUS expression was observed in all tissues and at all stages analyzed in the mutant (Supplemental Fig. 1b). The accumulation of cells expressing Arath;*CycB1*;1*:GUS* in the mutant suggests that a defective *FVE/MSI4* extends the duration during which cells are competent and/or continue to divide.

To confirm this hypothesis, we investigated the endoreduplication levels in leaves. In *Arabidopsis* leaf epidermal cells, the arrest of cell division is followed by the onset of endoreduplication with increased DNA content and usually cell expansion (Traas et al. 1998). Endoreduplication levels in leaves thus appear as an early marker of differentiation. The ploidy level was measured in expanded leaves of *fve-6* and wild type plants by flow cytometry (Fig. 4d). In *fve-6* leaves, the cells showed lower endo-reduplication levels since the proportion of 8C and 16C cells was reduced by 13%. These same leaves had sub-epidermal cells which were less vacuolated and contained smaller and more regularly shaped chloroplasts than the wild type, most likely corresponding to a less advanced differentiation stage (Fig. 4e, f).

Taken together, the results outline the role of *FVE/MSI4* in the regulation of the pattern of cell division/cell differentiation in lateral organs. This is achieved by *FVE/MSI4* controlling the switch or timing of proliferative cell growth to endoreduplication and differentiation during lateral organ growth. In the wild type, the amount of cell division is more restricted in space and time, while cellular differentiation through endoreduplication mechanism(s) is accelerated.

Connectivity between flowering time, meristem and organ growth

The question at this point was whether similar alterations occur in other late flowering mutants and whether *FVE/MSI4* control over *FLC*, the only known key-target of *FVE/MSI4,* could explain the observed changes produced at both meristem and organ growth levels.

Other late flowering mutants exhibit similar, though not identical, changes in rosette leaf number, plastochron and meristem size

Since mutations in *FVE/MSI4* primarily affected meristem activity, we tested whether similar alterations in meristem activities occur in other mutants with a late flowering phenotype (Table 3). Some of the corresponding genes are known as "floral pathway integrators" (Simpson and Dean 2002; Yu et al. 2002; Fig. 1). We show that these mutants tended to produce larger and more active inflorescence meristems than the wild type. However, no clear-cut correlations could be made between the gene position in the flowering network and meristem size and activity.

These results, together with the fact that *flc* mutants tend to flower only slightly earlier than the

Table 3 Effects of chosen mutations on flowering time (expressed in days and leaf number), plastochron and SAM size

Plant line	Flowering time (days)	Leaf number	Plastochron (leaves/week)	SAMi size (μm^2)
Ler	77	28.8 (2)	2.6	5,429 (1,015)
fve2	92	49.2 (5.6)	3.7	10,004 (1,540)
fca1	100	51.2 (5.4)	3.6	7,388 (1,093)
soc1	92	58.2 (4)	4.4	7,462 (1,203)
ft1	100	60.4 (2.4)	4.2	7,723 (436)
agl24	100	43.8 (5.7)	3.1	6,201 (2,300)
clv1-6	92	58.2 (9)	4.5	136,347 (27,800)

Experiments were performed in SD. Standard errors are given in brackets. *P*-values were highly significant for each mutant for leaf number. In the case of SAMi size, *P*-values were highly ($P < 0.001$; *fve2, clv1-6*) or very significant ($P < 0.01$; the other mutants), with the exception of *agl24*, in which case the *P*-value was not significant ($P = 0.5$)

corresponding wild type (Michaels and Amasino 1999; Takada and Goto 2003), suggested that the observed effects of mutations in *FVE/MSI4* cannot be entirely explained by the regulation of *FLC* alone. *FVE/MSI4* might therefore operate through additional targets with more general effects on development. Among the genes which were analyzed, two are reported here: *WUSCHEL (WUS)* and *TERMINAL FLOWER2 (TFL2/LHP1)*.

WUS expression profile in *fve-6* is similar to the wild type

We first wanted to test the possible role of *FVE/MSI4* in the control of stem cell domain activity. It has been established that the size and boundaries of the stem cell domain are constantly assessed and maintained through the size regulation of the *WUS* domain (Gross-Hardt and Laux 2003). We therefore analyzed by in situ hybridization the expression pattern of *WUS*, the major regulator of the stem-cell feedback loop. With its enlarged meristems, *fve-6* exhibited a proportionally enlarged *WUS* expression domain (Fig. 5d, f), with an expression pattern similar to the wild type (Fig. 5c, e). This was distinct from *WUS* patterns in *clv, fas* (*fasciated*) or *swp* (*struwwelpeter1*) mutant backgrounds (cf. Discussion).

The combined results on *WUS* expression, BrdU incorporation and plastochron data showed that larger apical meristems and increased organ number in the mutant could not simply result from a larger pool of stem cells, but depended on combined increased division rates in meristems and faster transit of the cells into the primordia, implying a more global and co-ordinated control on meristem activities by *FVE/MSI4*.

FVE/MSI4 is a negative regulator of *TFL2/LHP1* and *FLC* during development

We have chosen *TFL2/LHP1*, a chromatin remodeling factor, for further tests because *tfl2/lhp1* mutants have an opposite phenotype to *fve* (premature transition through phase changes, early flowering, non-branching shoots with 30–50% reduction in size and biomass, cell size alterations, etc. Gaudin et al. 2001; Larsson et al. 1998; Fig. 1). Also, the global expression data analysis we searched at https://www.genevestigator.ethz.ch/at/ (Digital Northern, Gene Chronologer, Gene Atlas and Meta Analyzer) indicated that *TFL2/LHP1* expression profiles tend to coincide with those of *FVE/MSI4* during the main stages of the life cycle. Last but not least, *TFL2/LHP1* has been reported to repress *FLC* (Mylne et al. 2006; Turck et al. 2007 for a summary) and *FT* (Kotake et al. 2003; Fig. 1).

Semi-quantitative RT-PCR tests were performed on RNA samples from wild type, *fve-6* and *lhp1* plants with primers for downstream genes such as *FLC, SOC1, FT* and *LFY* (Fig. 6a, b). In addition, we assessed the expression levels of *TFL2/LHP1* in *fve-6* mutant samples compared to wild type (Fig. 6c–e). Taken together, the results indicated that (1) maximum *FLC* repression required the combined activity of *FVE/MSI4* and *TFL2/LHP1* (i.e., in the wild type), with *FVE/MSI4* playing the main part in this repression (compare *FLC* levels in *fve-6* versus *lhp1*, Fig. 6a, b); (2) *TFL2/LHP1* was up-regulated (2.5-fold) in *fve-6* meristems, while *FVE/MSI4* levels

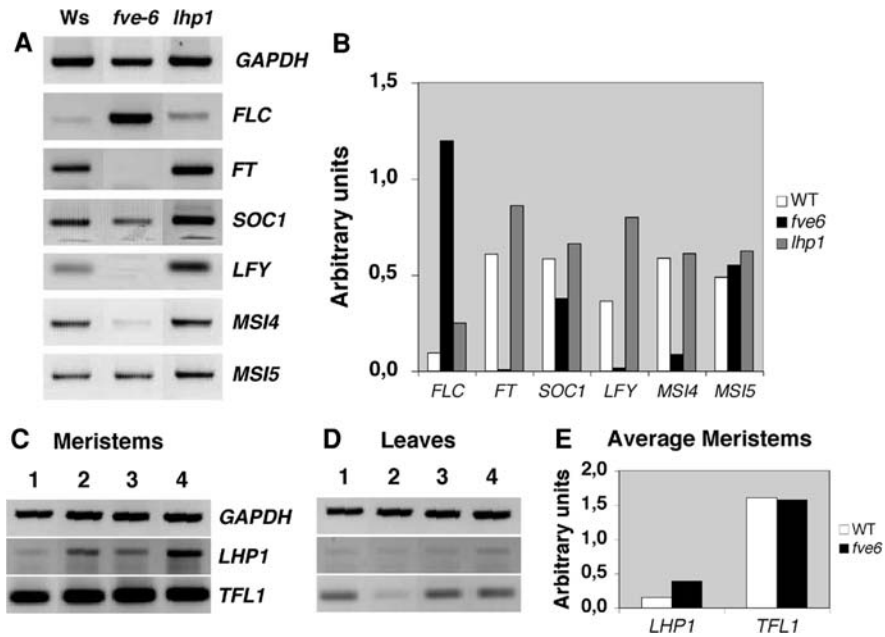

Fig. 6 Semi-quantitative RT-PCR transcript analysis in wild type and mutant backgrounds. **a** and **b** *FLC*, *FT*, *SOC1* and *LFY* RNA levels in W*s* (lane 1), *fve-6* (lane 2) and *lhp1* (lane 3) backgrounds, with *GAPDH* RNA as internal control and *FVE/MSI4* and *MSI5* RNAs as reference. Samples corresponding to apical meristems and very young leaves taken and analyzed at regular intervals during development (2, 4, 6, 8, 12 leaf-stages) and representative cases are illustrated. The plants were grown under short days. **b** Graph showing the relative expression of the above genes normalized to the *GAPDH* control. **c**–**e** *TFL2/LHP1* and *TFL1* (*TERMINAL FLOWER 1*) RNA levels in shoot apices or leaf samples in W*s* (lanes 1, 3) and *fve-6* (lanes 2, 4) backgrounds at 6 leaf (lanes 1, 2) and 12 leaf (lanes 3, 4) rosette stages, respectively. *TFL1* served as control based on the fact that *TFL1* and *TFL2/LHP1* have additive genetic effects on flowering time (Larsson et al. 1998) and that *tfl1* is not epistatic over *fve* and several other flowering time genes (Ruiz-Garcia et al. 1997). The plants were grown under short days. **c** Panel, apical meristem and very young leaves. **d** Panel, leaves. *GAPDH* RNA was amplified as internal control and *TFL1* RNAs were used as reference. **e** Graph showing the relative expression of the two genes normalized to the GAPDH control. The effective values for *LHP1* were 0.16 in the wild type and 0.39 in *fve-6*

appeared not to be altered in *lhp1* (Fig. 6a/c, b/e); (3) *FT* repression was highest when *TFL2/LHP1* was highest, i.e., in a *fve-6* background, indicating that *TFL2/LHP1* was a key regulator of *FT* in this context (Fig. 6b, e). Based on the above considerations, we concluded that *FVE/MSI4* acted as a repressor of *TFL2/LHP1* (Fig. 7). The analyzed *fve6* phenotype could therefore result from altered levels of both *FLC* and *TFL2/LHP1*.

We then tested at genetic level the relationship between *FVE/MSI4* and *TFL2/LHP1*. Two *tfl2/lhp1* alleles were crossed to *fve* in two different genetic backgrounds, namely *lhp1* to *fve-6* (in Ws) and *tfl2-3* to *fve-2* (in Ler). In F2, the double mutant had a phenotype very close, but not identical, to *lhp1/tfl2,* indicating that the epistasy of *tfl2/lhp1* over *fve-6/fve2* was not complete (Table 4). This suggested again that *FVE/MSI4* is an important, but not the only, *TFL2/LHP1* regulator.

That this is the case was further supported by the Mutant Surveyor dataset at https://www.genevestigator.ethz.ch/at/ (global expression profiles of 140 mutants) where pair-wise comparisons between *FVE/MSI4*, *TFL2/LHP1* and *FLC* were performed. First, these genes are part of shared epigenetic, cell division-cell differentiation and biotic and abiotic signaling networks (i.e. the level of expression of the three genes simultaneously varied in mutants affected, for example, in embryo maturation, in the retinoblastoma/E2F pathway or in temperature acclimation). Second, *LHP1/TFL2* clearly responded to certain mutant backgrounds (for example, in the *CTR1-EIN2* ethylene signaling and auxin transport and polarity control, or the Dicer-like and RDR epigenetic functions), while *FVE/MSI4* did not, and vice-versa (for example, micro-RNA—mediated gene silencing).

Finally, on the basis of the analyzed *FVE/MSI4*—*TFL2/LHP1* relationship, the connectivity between

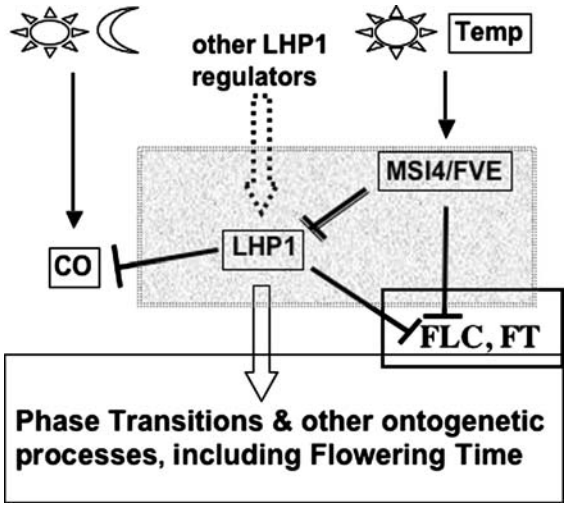

Fig. 7 Additional regulatory interactions of *FVE/MSI4* during flowering and development. *FVE/MSI4* is shown as a repressor of *TFL2/LHP1*. The proposed position of *TFL2/LHP1* in the network implies a flowering time network broadly open to the effects of additional internal and external cues (see Discussion). We hypothesize that *TFL2/LHP1* and *FVE/MSI4*, together with other factors, act to connect various developmental processes and phases during ontogenesis (shown as a *box*; also see Guyomarc'h et al. 2005; Reyes 2006)

Table 4 Flowering time at bolting expressed as leaf number in the F2 segregation population of the double *fve-2 tfl2-3* mutant

Plant line	Leaf number
WT	24.8 (2.3)
fve-2	43.3 (3.2)
tfl2-3	14.0 (1.3)
tfl2-3 fve-2	19.3 (2.7)

Experiments were performed in LD. *Standard error* is given in brackets. *P*-values were calculated in pair wise combinations and were very significant for the pairs wild type/*tfl2 fve* ($P = 0.0032$) and *tfl2*/*tfl2 fve* ($P = 0.0018$). *P*-values were highly significant ($P < 0.001$) in all the other cases

meristem activities, organ growth and flowering time could gain additional weight based on recently identified *TFL2/LHP1* targets. Global expression profiling (Nakahigashi et al. 2005) and ChIP-chip analysis (chromatin immunoprecipitation and hybridization to *Arabidopsis* chromosome 4 tilling array; Turck et al. 2007), indicated that the gene may affect as much as 10% of the *Arabidopsis* gene pool (as extrapolated by us from the reported 605 target genes on chromosome 4 alone). We mined the supplemental data (Table S2) in Turck et al. (2007) and classified the *TFL2/LHP1* target genes in meristem and primordia function regulators (*KNAT1, AGO1*, *NAM*- and *TFL1*-like, *LFY, ANT* genes), organ identity, growth and polarity factors in leaf and flower development (several *MADS*-box, *YABBY, LOB, ARF* and *AUX/IAA, MYB, RLK* genes, to name just a few) and flowering time control (*FT, FLC, FLF* genes).

On the basis of all the above results, we hypothesize that *FVE/MSI4* operates in a broader developmental context than reported before, which is sketched in Fig. 7.

Discussion

The histone chaperone *FVE/MSI4* (Ausin et al. 2004) was identified genetically as a member of the autonomous pathway corresponding to the *fve* locus (Martinez-Zapater and Somerville 1990; Koornneef et al. 1991). The gene is highly conserved in eukaryotes (Ach et al. 1997; Hennig et al. 2003).

By using combined morphological, genetic, molecular and cytological approaches, we investigated the pleiotropic effects of mutations in *FVE/MSI4* on plant morphogenesis. The gene is present in all cells, the protein has a nuclear localization (Delichère et al. 1999; Ach et al. 1997) and is rate limiting in the cell. Table 5 summarizes the extent of overall morphological changes at various levels of organization in the mutant. The main trends clearly show the major involvement of *FVE/MSI4* in meristem regulatory activities (for example, size modifications by a factor 2–3) and more modest effects on organ growth control (for example, cell number modification by a factor 1.25–1.5). Overall, combined data from Table 2 indicate an effective vegetative biomass enhancement in the mutants of three- to eightfold.

FVE/MSI4 and meristem functions

Concerning meristem functions, the combined results on *FVE/MSI4* and *WUS* expression patterns, meristem size measurements and BrdU incorporation data, demonstrated that an impaired *FVE/MSI4* resulted in faster cell proliferation in shoot meristems coupled with faster rates of cell exit to differentiation (accelerated plastochron) in *fve-6*. Table 5 shows that these components of SAM activity have been co-ordinately upgraded in the mutant. This is different from meristem

Table 5 An overview of morphological changes measured at organ and cellular levels (number and size) in wild type and *fve-6* mutant aiming to illustrate the differential effects of *FVE/MSI4* on meristem activity and organ growth during the vegetative and reproductive phases

Organ type	Organ level		Cellular level		Observations and growth compensation
	Number	Size	Number	Size	
SAMv	Leaf	Leaf	Leaf	Leaf	Stem cell homeostasis up-grade
Area 2×	2–3×	1.25×	1.5×	0.8×	Faster plastochron
AD, Less in wt.					Partial compensation for cell number/size in leaves
SAMi	FM	FM	FM	FM	Stem cell homeostasis up-grade
Area 3×	2× (a)	3×	1.25×	1.2×	No compensation of cell number/size in FM
AD, more in wt.					
Flower	Petal	Petal	Petal	Petal	No compensation of cell number/size in petals
	(b)	1.5×	1.2×	1.3×	

The differences are expressed as fold-increase in the mutant with wild type values taken as 1

AD stands for Apical Dominance. It is expressed during the vegetative phase as axillary shoot formation and during the reproductive phase as secondary inflorescence formation

FM, floral meristem; SAMi, shoot apical meristem at inflorescence stage; SAMv, shoot apical meristem at vegetative stage

(a) As silique number; (b) Occasionally more than four petals

mutants such as *clv, fas* and *swp1* (Schoof et al. 2000; Kaya et al. 2001; Autran et al. 2002). For example, *clv* mutants have a massive SAM resulting from a delay in transition from stem cell to organ forming domains (Clark et al. 1993), while *fas* mutants have altered organ initiation per se (Vernoux et al. 2000). These facts taken together, we concluded that the function of *FVE/MSI4* is to scale-down meristem activities, speed up the transition to the reproductive phase and accelerate organ differentiation during adult stages.

FVE/MSI4 and organ growth

What is the relative contribution of changes in organ number and organ growth to biomass increase in the mutants? Our results show a doubling-to-tripling of leaf number in the mutants and a corresponding increase in vegetative biomass is a reasonable estimate. By deduction, changes in leaf growth control due to mutations in *FVE/MSI4* would, at least under LD cultivation, contribute by an equivalent factor to the overall increase in vegetative biomass. *FVE/MSI4* regulates organ growth by controlling the timing of cell proliferation/cell differentiation transition. For example, *fve-6* leaves had an altered timing of growth phases with effects on cell number and cell size. This regulatory role appeared to operate through a combined control on cell proliferation and endoreduplication. The results raise the question of growth compensation mechanisms (reviewed in Doonan 2000; Tsukaya 2003), which have been reported in loss-of-function (for example *ant*), or gain-of-function (for example several cell cycle genes) gene alterations. We show that alterations in *FVE/MSI4* generated differential compensation responses in different organ types (also see Hafen and Stocker 2003) and that such compensations were not automatic. Thus, mutual compensation mechanisms of the "total checkpoint mass" hypothesis (Doonan 2000) were not effective in the case of *FVE/MSI4*. This appears to be also the case with other genes acting as phase change regulators such as *SWP1* (Autran et al. 2002), *ARGONAUTE* (*AGO1*, Morel et al. 2002), a protein involved in PTGS, or *HASTY* (*HST*, Bollman et al. 2003), an ortholog of *exportin5/MSN5*.

Beyond the autonomous pathway and flowering time—*FVE/MSI4* plays extended roles in development

We infer from the above that *FVE/MSI4* is a general developmental regulator operating through multilevel and multifactor controls, which translate meristem activities and organ growth processes into more integrated developmental decisions. The fact that *fve-6* exhibits pleiotropic modifications at the level of plant architecture, organ and cell growth at all stages of development, speaks in favor of this interpretation.

Our preliminary work on other late flowering mutants suggests that flowering time network integrators are interconnected with meristem factors, indicating coordinated roles in the progression through developmental stages, of which flowering time is a conspicuous component. The possibility that the autonomous pathway genes play earlier and much wider roles in development has been suggested earlier (Schultz and Haughn 1993; Martinez-Zapater et al. 1995; Simpson and Dean 2002), and gained recent experimental support through work on *FY* allelic series (embryo development; Henderson et al. 2005), but also on *FCA* and *FPA* genes (RNA-mediated chromatin silencing; Baürle et al. 2007).

Concerning *FVE/MSI4,* we demonstrate that defined cellular processes can be linked to the molecular and genetic aspects of flowering time control. In addition, the identification of *TFL2/LHP1*, a highly conserved global regulator of development, as an additional target of *FVE/MSI4*, is an important finding as it sets the regulatory role of *FVE/MSI4* in a much broader context. *LHP1/TFL2* is a Heterochromatin Protein1 homolog involved in the epigenetic control of euchromatin transcription. As a chromatin remodeling factor, the gene controls developmental transitions during ontogenesis, while affecting flowering time (Reyes 2006; Guyomarc'h et al. 2005; Steiner et al. 2004).

The repression exerted by *FVE/MSI4* on *TFL2/LHP1* is expected to release at least partly a large set of its targets which control meristem activities, flower organ identity, meiosis, seed maturation (Nakahigashi et al. 2005; Turck et al. 2007; also see Reyes 2006). This results in the acceleration of ontogenesis (both during vegetative and reproductive phases) and effective flower formation. We therefore propose that the balance of these two chromatin factors and more general gene regulators plays an important role in calibrating ontogenesis (Fig. 7).

Since *FVE/MSI4* also plays a flowering time-independent, "thermosensing" role for both ambient temperature and intermittent cold (Blazquez et al. 2003; Kim et al. 2004), the gene operates as a tuning factor, rather than an ON–OFF switch, to modulate the ontogenetic dynamics by integrating several external and internal cues primarily at the SAM. In the light of these facts, we argue that the primary function of *FVE/MSI4* might be the dynamic organization of chromatin rather than regulatory functions per se. Bäurle and Dean (2006) raise similar issues with reference to other mutants altered in developmental transitions (also see Guyomarc'h et al. 2005; Reyes 2006).

Whatever the primary role of *FVE/MSI4*, mutations in the gene resulted in the recalibration of many developmental parameters with no morphological abnormalities *stricto sensu* being produced, except that the mutants lived on average twice as long as the wild type and produced a spectacular increase in biomass. Total biomass and grain production (yield) increase have been a constant challenge in plant breeding and represent the main trends in *fve* mutants. Of note, QTL mapping and cloning for yield or growth in maize, rice, wheat or *Arabidopsis* (Zhang 2007; Shindo et al. 2007; Quarrie et al. 2006; Koorneeff et al. 2004) have not identified *FVE/MSI4* among candidate genes. According to our preliminary results, allelic and ecotypic variations in *FVE/MSI4* alterations tend to be low, suggesting that only weak modifiers have evolved for this essential gene. Genes of the kind deserve particular attention in plant breeding as they are likely to become tools in biotech for engineering biomass (for food, feed, green manure) and adjusting life-cycle to climate change conditions (for example in regions which undergo an extension of vegetation and/or rain seasons), while facing the triple demographic, environmental and deforestation challenge (Rothstein 2007). Finally and from a more fundamental point of view, our experiments underline the surprising potential of *Arabidopsis* to modulate its lifespan on a broad scale, far beyond the capacity of known animal models (Weil and Radman 2004).

Acknowledgments We are much indebted to Anne-Marie Thierry, Alexis Lacroix, Pierre Chambrier, Sandrine Mouradian-Garcia for their excellent technical assistance, to Valerie Gaudin, Dirk Inzé, Yu Hao and Jan Traas for making available mutant and reporter lines and to Ottoline Leyser, Caroline Dean, Françoise Monéger, Jan Traas, François Parcy, Soazig Guyomarc'h and Jonathan Fitzgerald for critically reading this manuscript. Last but not least, the authors are indebted to anonymous reviewers for helpful criticism and suggestions.

References

Ach RA, Taranto P, Gruissem W (1997) A conserved family of WD-40 proteins binds to the retinoblastoma protein in both plants and animals. Plant Cell 9:1595–1606

Ausin I, Alonso-Blanco C, Jarillo JA, Ruiz-Garcia L, Martinez-Zapater JM (2004) Regulation of flowering time by FVE,

a retinoblastoma-associated protein. Nat Genet 36:162–166. doi:10.1038/ng1295
Ausubel FM, Brent R, Kinston RE, Moore DD, Seidmann IG, Smith JA et al (1993) Current protocols in molecular biology. Wiley, New York
Autran D, Jonak C, Belcram K, Beemster GT, Kronenberger J, Grandjean O et al (2002) Cell numbers and leaf development in *Arabidopsis*: a functional analysis of the *STRUWWELPETER* gene. EMBO J 21:6036–6049. doi:10.1093/emboj/cdf614
Bäurle I, Dean C (2006) The timing of developmental transitions in plants. Cell 125:655–664. doi:10.1016/j.cell.2006.05.005
Baürle I, Smith L, Baulcombe D, Dean C (2007) Widespread role for the flowering time regulators FCA and FPA in RNA-mediated chromatin silencing. Science 318:109–112. doi:10.1126/science.1146565
Bechtold N, Ellis J, Pelletier G (1993) In planta *Agrobacterium* mediated gene transfer by infiltration of adult *Arabidopsis thaliana* plants. C R Acad Sci Paris 316:1194–1199
Becker D, Kemper E, Schell J, Masterson R (1992) New plant binary vectors with selectable markers located proximal to the left T-DNA border. Plant Mol Biol 20:1195–1197. doi:10.1007/BF00028908
Blazquez M, Ahn JH, Weigel D (2003) A thermosensory pathway controlling flowering time in *Arabidopsis thaliana*. Nat Genet 33:168–171. doi:10.1038/ng1085
Bollman KM, Aukerman MJ, Park M-Y, Hunter C, Berardini TZ, Peothig RC (2003) HASTY, the *Arabidopsis* ortholog of exportin 5/MSN5, regulates phase change and morphogenesis. Development 130:1493–1504. doi:10.1242/dev.00362
Clark S, Running MP, Meyerowitz EM (1993) *CLAVATA1*, a regulator of meristem and flower development in *Arabidopsis*. Development 119:397–418
Colon-Carmona A, You R, Haimovitch-Gal T, Doerner P (1999) Technical advance: spatio-temporal analysis of mitotic activity with a labile cyclin-GUS fusion protein. Plant J 20:503–508. doi:10.1046/j.1365-313x.1999.00620.x
de Almeida Engler J, De Groodt R, Van Montagu M, Engler G (2001) In situ hybridization to mRNA of *Arabidopsis* tissue sections. Methods 23:325–334. doi:10.1006/meth.2000.1144
Delichère C, Veuskens J, Hernould M, Barbacar N, Mouras A, Negrutiu I et al (1999) *SlY1*, the first active gene cloned from a plant Y chromosome, encodes a WD-repeat protein. EMBO J 18:4169–4179. doi:10.1093/emboj/18.15.4169
Doonan J (2000) Social control on cell proliferation in plants. C O Plant Biol 3:482–487. doi:10.1016/S1369-5266(00)00117-5
Ferreira PC, Hemerly AS, Engler JD, van Montagu M, Engler G, Inze D (1994) Developmental expression of the *Arabidopsis* cyclin gene *Cyc1At*. Plant Cell 6:1763–1774
Galbraith W, Wagner MC, Chao J, Abaza M, Ernst LA, Nederlof MA et al (1991) Imaging cytometry by multiparameter fluorescence. Cytometry 12:579–596. doi:10.1002/cyto.990120702
Gaudin V, Libault M, Pouteau S, Juul T, Zhao G, Lefebvre D et al (2001) Mutations in *LIKE HETEROCHROMATIN PROTEIN 1* affect flowering time and plant architecture in *Arabidopsis*. Development 128:4847–4858
GENEVESTIGATOR v3 (2007) ETH Zürich, at https://www.genevestigator.ethz.ch/at/
Gross-Hardt R, Laux T (2003) Stem cell regulation in the shoot meristem. J Cell Sci 116:1659–1666
Guyomarc'h S, Bertrand C, Delarue M, Zhou DX (2005) Regulation of meristem activity by chromatin remodelling. Trends Plant Sci 10:332–338
Hafen E, Stocker H (2003) How are the sizes of cells, organs, and bodies controlled? PLoS Biol 1:E86
He Y, Amasino RM (2005) Role of chromatin modification in flowering-time control. Trends Plant Sci 10:30–35
Hemerly AS, Ferreira PC, de Almeida Engler J, Van Montagu M, Engler G, Inzé D (1993) cdc2a expression in *Arabidopsis* is linked with competence for cell division. Plant Cell 12:1711–1723
Hemerly AS, Ferreiera PC, Van Montagu M, Inzé D (1999) Cell cycle control and plant morphogenesis: is there an essential link? BioEssays 21:29–37
Henderson IR, Liu F, Drea S, Simpson GG, Dean C (2005) An allelic series reveals essential roles for FY in plant development in addition to flowering-time control. Development 132:3597–3607
Hennig L, Taranto P, Walser M, Schonrock N, Gruissem W (2003) *Arabidopsis* MSI1 is required for epigenetic maintenance of reproductive development. Development 130:2555–2565
Jack T (2004) Molecular and genetic mechanisms of flower control. Plant Cell 16:S1–S17
Kaya H, Shibahara KI, Taoka KI, Iwabuchi M, Stillman B, Araki T (2001) *FASCIATA* genes for chromatin assembly factor-1 in *Arabidopsis* maintain the cellular organization of apical meristems. Cell 104:131–142
Kim HJ, Hyun Y, Park J-Y, Park M-J, Kim MD, Kim H-Y, Lee MH, Moon J, Lee I, Kim J (2004) A genetic link between cold responses and flowering time through *FVE* in *Arabidopsis*. Nat Genet 36:167–171
Kobayashi Y, Kaya H, Goto K, Iwabuchi M, Araki T (1999) A pair of related genes with antagonistic roles in mediating flowering signals. Science 286:1960–1962
Komeda Y (2004) Genetic regulation of time to flower in *Arabidopsis thaliana*. Annu Rev Plant Biol 55:521–535
Koornneef M, Hanhart CJ, van der Veen JH (1991) A genetic and physiological analysis of late flowering mutants in *A. thaliana*. Mol Gen Genet 229:57–66
Koorneeff M, Alonso-Blanco C, Vreugdenhil D (2004) Naturally occurring genetic variation in *Arabidopsis thaliana*. Annu Rev Plant Biol 55:141–172
Kotake T, Takada S, Nakahigashi K, Ohto M, Goto K (2003) *Arabidopsis TERMINAL FLOWER 2* gene encodes a heterochromatin protein 1 homolog and represses *FLOWERING LOCUS T* to regulate flowering time and several flowering homeotic genes. Plant Cell Physiol 44:555–564
Krizek BA, Fletcher JC (2006) Molecular mechanisms of flower development: an armchair guide. Nature Rev Genet 6:688–698
Larsson AS, Landberg K, Meeks-Wagner DR (1998) The *TERMINAL FLOWER 2* (*TFL2*) gene controls the reproductive transition and meristem identity in *Arabidopsis thaliana*. Genetics 149:597–605
Lentner C (1982) Geigy scientific tables. Ciba-Geigy, Basel
Martinez-Zapater JM, Somerville CR (1990) Effect of light quality on late flowering mutants of *Arabidopsis thaliana*. Plant Physiol 92:770–776

Martinez-Zapater J, Jarillo JA, Cruz-Alvarez M, Roldan M, Salinas J (1995) *Arabidopsis* late flowering *five* mutants are affected in both vegetative and reproductive development. Plant J 7:543–551

Meyerowitz EM (1997) Genetic control of cell division patterns in developing plants. Cell 88:299–308

Michaels SD, Amasino RM (1999) *FLOWERING LOCUS C* encodes a novel MADS domain protein that acts as a repressor of flowering. Plant Cell 11:949–956

Michaels SD, He Y, Scortecci KC, Amasino RM (2003) Attenuation of *FLC* activity as a mechanism for the evolution of summer-annual flowering behaviour in *Arabidopsis*. Proc Natl Acad Sci USA 100:10102–10107

Mizukami Y, Fischer RL (2000) Plant growth size control: *AINTEGUMENTA* regulates growth and cell numbers during organogenesis. Proc Natl Acad Sci USA 97:942–947

Morel JB, Godon C, Mouirrain P, Beclin C, Boutet S, Feuerbach F, Proux F, Vaucheret H (2002) Fertile hypomorphic *ARGONAUTE* (*ago1*) mutants impaired in PTGS and virus resistance. Plant Cell 14:629–639

Mouradov A, Cremer F, Coupland G (2002) Control of flowering time: interacting pathways as a basis for diversity. Plant Cell 14(suppl):S111–S130

Mylne JS, Barret L, Tessadori F, Mesnage S, Johnson L, Bernatavichute YV, Jacobsen SE, Fransz P, Dean C (2006) LHP1, the Arabidopsis homologue of HETEROCHROMATIN PROTEIN1, is required for epigenetic silencing of FLC. Proc Natl Acad Sci USA 103:5012–5017

Nakahigashi K, Jasenkakova Z, Schubert I, Goto K (2005) The Arabidopsis heterochromatin protein 1 homolog (TERMINAL FLOWER2) silences genes within the euchromatic region but not genes positioned in heterochromatin. Plant Cell Physiol 46:1747–1756

Quarrie SA, Quarrie SP, Radosevic R, Rancic D, Kaminska A, Barnes JD, Leverington M, Ceoloni C, Dodig D (2006) Dissecting a wheat QTL for yield present in a range of environments: from QTL to candidate genes. J Exp Botany 57:2627–2637

Quesada V, Dean C, Simpson GG (2005) Regulated RNA processing in the control of Arabidopsis flowering. Int J Dev Biol 49:773–780

Reyes JC (2006) Chromatin modifiers that control plant development. CO Plant Biology 9:21–27

Rothstein SJ (2007) Returning to our roots: making plant biology research relevant to future challenges in agriculture. Plant Cell 19:2695–2699

Ruiz-Garcia L, Madueno F, Wilkinson M, Haughn G, Salinas J, Martinez-Zapater JM (1997) Different roles of flowering time genes in the activation of floral initiation genesin *Arabidopsis*. Plant Cell 9:1921–1934

Samach A, Onouchi H, Gold ES, Ditta GS, Schwart-Sommer Z, Yanofsky MF, Coupland G (2000) Distinct roles of *CONSTANS* target genes in reproductive development of *Arabidopsis*. Science 288:1613–1616

Schoof H, Lenhard M, Haecker A, Mayer FK, Jurgens G, Laux T (2000) The stem cell population of *Arabidopsis* shoot meristem is maintained by a regulatory loop between *CLAVATA* and *WUSCHEL* genes. Cell 100:635–644

Schultz EA, Haughn GW (1993) Genetic analysis of the floral initiation process (FLIP) in *Arabidopsis*. Development 119:745–765

Sharma VK, Fletcher JC (2002) Maintenance of shoot and floral meristem cell proliferation and fate. Plant Physiol 129:31–39

Shindo C, Bernasconi G, Hardtke CS (2007) Natural genetic variation in Arabidopsis: tools, traits and prospects for evolutionary ecology. Ann Botany 99:1043–1054

Simpson GG (2004) The autonomous pathway: epigenetic and post-transcriptional gene regulation in the control of Arabidopsis flowering time. Plant Biol 7:570–574

Simpson GG, Dean C (2002) *Arabidopsis*, the Rosetta stone of flowering time? Science 296:285–289

Steiner A, Schöb H, Grossniklaus U (2004) Epigenetic control of plant development: new layers of complexity. C O Plant Biol 7:11–19

Takada S, Goto K (2003) TERMINAL FLOWER 2, an *Arabidopsis* homolog of HETEROCHROMATIN PROTEIN 1, counteracts the activation of *FLOWERING LOCUS T* by CONSTANS in the vascular tissues of leaves to regulate flowering time. Plant Cell 15:2856–2865

Traas J, Hulskamp M, Gendreau E, Hofte H (1998) Endoreduplication and development: rule without dividing? C O Plant Biol 1:498–503

Tsukaya H (2003) Organ shape and size: a lesson from studies of leaf morphogenesis. C O Plant Biol 6:57–62

Turck F, Roudier F, Farrona S, Martin-Magniette M-L, Guillaume E, Buisine N, Gagnot S, Martienssen RA, Coupland G, Colot V (2007) Arabidopsis TFL2/LHP1 specifically associates with genes marked by trimethylation of histone H3 Lysine27. PloS Genet 3:855–866

Vernoux T, Autran D, Traas J (2000) Developmental control of cell division patterns in the shoot apex. Plant Mol Biol 43:569–581

Weil J-C, Radman M (2004) How good is our genome? Phil Trans R Soc Lond B 359:95–98

Yu L, Gaitatzes C, Neer E, Smith TF (2000) Thirty-plus functional families from a single motif. Protein Sci 9: 2470–2476

Yu H, Xu Y, Tan EL, Kumar PP (2002) *AGAMOUS-LIKE 24*, a dosage-dependent mediator of the flowering signals. Proc Natl Acad Sci USA 99:16336–16341

Zhang K (2007) Strategies for developing green super rice. PNAS 104:16402–16409

Zimmermann P, Hirsch-Hoffmann M, Hennig M, Gruissem W (2004) GENEVESTIGATOR, *Arabidopsis* microarray database and analysis toolbox. Plant Physiol 136:2621–2632